Sensitivity and detection limits of MRI, CT and SPECT for Holmium-loaded microspheres

P. R. Seevinck[1], J-H. Seppenwoolde[1], T. C. de Wit[2], J. F. Nijsen[2], F. J. Beekman[2], A. D. van het Schip[2], C. J. Bakker[1]

[1]Image Sciences Institute, University Medical Center, Utrecht, Netherlands, [2]Department of Nuclear Medicine, University Medical Center, Utrecht, Netherlands

Introduction

A distinct trend in image-guided treatment is the integration of imaging modalities and the development of dedicated multimodal diagnostic and therapeutic agents [1]. A therapeutic anticancer agent with multimodal imaging opportunities, viz. Holmium-loaded microspheres (HoMS), was developed by our group [2]. To investigate the possible role of this agent in the diagnostic workup and treatment of cancerous disease, more insight is needed in the performance of the agent as a multimodal diagnostic agent. HoMS has great potential as a therapeutic agent for internal radionuclide therapy of tumors since activated HoMS (Ho-166) emits high-energy β-particles. Besides that, HoMS contains the properties to become a truly multimodal diagnostic agent since it is strongly paramagnetic (MRI), has a high linear attenuation coefficient (CT) and, when activated, emits γ-rays visible with SPECT.

In this work, we studied the diagnostic potential of HoMS as a multimodal contrast agent, and therefore, crucial parameters concerning low contrast detectability (sensitivity and detectability) were determined on clinical CT, MRI and SPECT scanners. Phantom experiments were conducted using straightforward clinical scan protocols and basic performance evaluation procedures. For each modality, the signal change as a function of the HoMS concentration was measured, from which the sensitivity and low contrast detectability were calculated.

Materials and Methods

HoMS: HoMS was prepared by solvent evaporation, resulting in a size distribution of 20-50 µm and a Holmium content of 17 % by weight. Activation for SPECT imaging was achieved by neutron bombardment, resulting in an activated fraction of 1.5 ppm Ho-166 (γ-rays: 80.6 keV (6.7%); β-particles: E_{max}=1.77 MeV (49%)/ 1.85 MeV (50%); $t_{1/2}$=26.8h) [3]. *Samples:* Duplicate samples with HoMS concentrations ranging from 0 to 10 mg/ml were obtained by dissolving HoMS in a 2% agar gel. Samples were sealed in tubes with a diameter of 2.2 cm and a length of 7.0 cm. *Phantom setup:* Each sample was positioned co-axially in a cylindrical phantom (inner diameter 21.6 cm, inner height 18.6cm) and measured individually. *Imaging parameters: MRI*: Experiments were done on a 1.5 T whole-body scanner (Achieva, Philips Medical Systems, Best, NL). $T2^*$-weighted images were obtained with a multi-echo gradient-echo sequence with 15 echoes at equal intervals of 1.23ms. Other imaging parameters included: TR/TE=31/11ms; flip=25º; FOV=256x256mm^2; matrix=192x192; NSA=8; slice thickness=10mm; total scan time=69s. This scan protocol represents a typical T2*- weighted sequence for detecting T2* modifying agents [4] *CT*: Experiments were done on a clinical CT scanner (Brilliance, Philips Medical Systems, Best, NL). Imaging parameters included a FOV of 350x350mm^2, matrix=512x512, collimation of 32x1.25mm, slice thickness of 3mm, pitch=0.671, rotation time=0.75s and total imaging time=2.82s. X-ray tube settings were 120kV and 200mAs. A soft tissue reconstruction filter was used. *SPECT*: Experiments were done on a clinical dual-head SPECT scanner (ADAC Vertex, Philips Medical Systems, Best, NL). A medium energy general purpose (MEGP) collimator was used. A 15% wide energy window was set around the Ho-166 photopeak at 81keV. Other imaging parameters included: matrix=128x128, projection pixel and reconstructed voxel size=4.72^{3}mm^3, 2 detector heads at 180º, 30 angular positions over 360º, 40 s per angle, resulting in a total scan time of 24min. No attenuation correction was applied. Reconstruction was done iteratively (n=12), using a Butterworth filter of order 5 with cut-off frequency=0.5. *Data analysis:* Data analysis was performed on ROI data covering the area of the sample (3.8cm^2). A slice thickness of 1 cm was analyzed. Calibration curves for each modality were obtained by linear regression analysis of ROI data from the reconstructed images for CT and SPECT and from the calculated R_2^* maps for MRI. For MRI, CT and SPECT the signal (S) is represented by R_2^* [s^{-1}], CT-value [HU] and intensity [a.u.], respectively. SPECT sensitivity is proportional to activity [Bq]. The sensitivity (dS/d[HoMS]) of each imaging modality was derived from the slope of the calibration curves. Contrast-to-noise ratios (CNR) were calculated for each modality for the ROI data relative to the background noise: CNR=($\Delta S_o/\sigma$). The minimum HoMS concentration (Dmin) was determined using a low contrast detectability criterion of a homogeneous object of A pixels: k<CNR.sqrt(A). A detection threshold of k=5 is generally accepted [5]. Since we assume low contrast, the noise amplitude in the object and background were assumed to be equal.

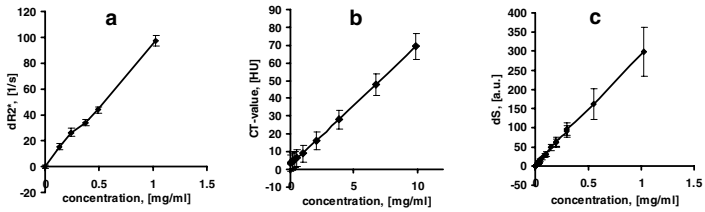

Fig. 1: Calibration curves of HoMS for MRI (a), CT (b) and SPECT (c). Error bars represent the standard deviation within the ROI.

Results

An excellent linear relationship between signal change and HoMS concentration was measured for all imaging modalities, as shown in Figure 1. SPECT turned out to yield the largest sensitivity, (316±1.9)au•ml•mg^{-1}, and the highest low contrast detectability, D_{min_SPECT}=0.006mg/ml. For MRI a sensitivity of (87.3±3.2)s^{-1}•ml•mg^{-1} was found and a low contrast detectability of D_{min_MRI}=0.02mg/ml. CT appeared to have the lowest sensitivity, (6.66±0.06)HU•ml•mg^{-1}, and the lowest low contrast detectability, D_{min_CT}=0.12mg/ml. The temporal resolution was highest for CT with 2.8s, compared to 69s for MRI and 24min for SPECT. The results are summarized in table 1, as well as other relevant imaging parameters.

Table 1: Summary of relevant parameters for MRI, CT and SPECT.

Modality	Pixel size (mm)	Noise level[1]	ROI (pix.)	Imaging time	Sensitivity[2] ([dS.ml.mg^{-1}])	D_{min}[1,2] (mg.ml^{-1})
MRI	1.33x1.33	2.5 s^{-1}	177	69 s	87.3±3.2 s^{-1}•ml•mg^{-1}	0.02
CT	0.68x0.68	4.7 HU	812	2.8 s	6.66±0.1 HU•ml•mg^{-1}	0.12
SPECT	4.72x4.72	0.3 a.u.	24	24 min	316±1.9 au•ml•mg^{-1}	0.006

[1] Normalized to 1 cm slice thickness; [2] Valid for an activated fraction of 1.5 ppm Ho-166.

Discussion and conclusions

Results were obtained with standard clinical imaging protocols and reconstruction algorithms and provided a first comparison of the potential of the different imaging modalities. The experimental setup met the signal-known-exactly, background-known-exactly criteria. Different experimental setups as well as optimization procedures could lead to different outcomes. The low therapeutic activated fraction of 1.5 ppm has no influence on detectability for MRI and CT. However, a higher activated fraction would lead to a dramatic further increase in sensitivity of SPECT relative to MRI and CT. The high resolution of CT positively influenced its low contrast detectability. Furthermore, CT allowed determining high concentrations of HoMS, where MRI and SPECT met difficulties, because of fast signal decay caused by an increased relaxivity and detector saturation caused by dead-time effects, respectively.

In conclusion, our phantom experiments clearly show that the presence of HoMS can be detected with three different modalities, albeit with very different sensitivity. SPECT is the most sensitive imaging modality for HoMS, but other parameters such as object size, contrast, and noise amplitude play an important role in the assessment of low contrast detectability as well. Which combination of modalities is most suitable depends on the specific task at hand, the signals from background and surrounding tissues as they occur in more realistic situations, the spatial and temporal resolution needed, and the fraction of activated Holmium.

References: [1] Zielhuis SW, CMC-ACA, 3:303-313 (2005)**;** [2] Nijsen JF, EJNM, 26:699-704 (1999); [3] Nijsen JFW, Biomaterials, 23:1831-839 (2002); [4] Dahnke H, MRM, 53:1202-1206 (2005), [5] Rose A, J. Opt. Soc. Am., 38:196-208 (1948).